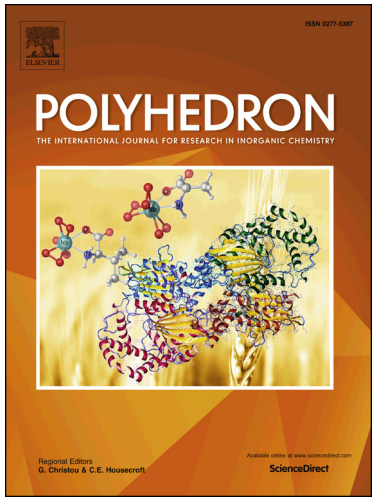

Coordination mode of the *N*-[bis(diethylamino)phosphoryl]benzenesulfonamide ligand in Lu(III) and Ag(I) complexes. Mass spectra, thermal properties and DFT calculations

Iuliia O. Shatrava, Vladimir A. Ovchynnikov, Kateryna E. Gubina, Tetyana Yu. Sliva, Olga V. Severinovskaya, Anatoliy G. Grebenyuk, Svitlana V. Shishkina, Vladimir M. Amirkhanov

PII: S0277-5387(17)30615-0
DOI: https://doi.org/10.1016/j.poly.2017.09.038
Reference: POLY 12848

To appear in: *Polyhedron*

Received Date: 18 July 2017
Accepted Date: 13 September 2017

Please cite this article as: I.O. Shatrava, V.A. Ovchynnikov, K.E. Gubina, T. Yu. Sliva, O.V. Severinovskaya, A.G. Grebenyuk, S.V. Shishkina, V.M. Amirkhanov, Coordination mode of the *N*-[bis(diethylamino)phosphoryl]benzenesulfonamide ligand in Lu(III) and Ag(I) complexes. Mass spectra, thermal properties and DFT calculations, *Polyhedron* (2017), doi: https://doi.org/10.1016/j.poly.2017.09.038

Coordination mode of the *N*-[bis(diethylamino)phosphoryl]benzenesulfonamide ligand in Lu(III) and Ag(I) complexes. Mass spectra, thermal properties and DFT calculations

Iuliia O. Shatrava[1*], Vladimir A. Ovchynnikov[1], Kateryna E. Gubina[1], Tetyana Yu. Sliva[1], Olga V. Severinovskaya[2], Anatoliy G. Grebenyuk[2], Svitlana V. Shishkina[3,4] and Vladimir M. Amirkhanov[1]

1 Department of Chemistry, Taras Shevchenko National University of Kyiv, 64/13, Volodymyrska Str., Kyiv 01601, Ukraine
2 Chuiko Institute of Surface Chemistry of National Academy of Sciences of Ukraine, 17 General Naumov Str., Kyiv, 03164, Ukraine
3 SSI "Institute for Single Crystals", National Academy of Science of Ukraine, 60, Nauky Ave., Kharkiv 61001, Ukraine
4 Department of Inorganic Chemistry, V. N. Karazin Kharkiv National University, 4 Svobody sq., Kharkiv 61077, Ukraine

Keywords: Crystal structure; lutetium(III); silver(I); laser desorption/ionization (LDI MS); DFT calculations.

Abstract

The sulfonylamidophosphate ligand $C_6H_5SO_2NHPO(N(C_2H_5)_2)_2$ (HL) has been used for the synthesis of two novel complexes: LuL_3 (**1**) and $(AgL)_n$ (**2**). According to an X-ray diffraction study, in the structure of HL, the molecules are linked into polymeric chains by strong N-H···O=P hydrogen bonds. The three acido-ligands ($\mathbf{L}^-$) in the structure of **1** are coordinated to the lutetium ion in a bidentate-chelate manner *via* two oxygen atoms of the phosphoryl and sulfonyl groups, forming six-membered metallocycles, which adopt a boat conformation. In the structure of **2**, the ligand is coordinated in the bidentate-bridging mode *via* the oxygen atom of the phosphoryl group and the nitrogen atom of the imide group; the chelate adopts a twist-boat conformation. The thermal behavior of the complexes **1** and **2** was studied by means of TG analysis. Results of IR-spectroscopy and LDI, ESI MS are discussed and compared with those obtained from DFT calculations.

1. Introduction

Progress in coordination chemistry allows the development of novel compounds which may be used as metallo-drugs, with directed and preset properties. Attention to coordination chemistry of polyfunctional phosphorus compounds has recently grown due to the application of such compounds as extractants [1], urease inhibitors, enzyme inhibitors, potential antiviral and anticancer drugs [2]. Among them, CAPhs (carbacylamidophosphates) are interesting and promising compounds to study: containing the structural fragment C(O)NHP(O), CAPhs can be considered as P, N structural analogues of the well-known β-diketones. The presence of the phosphoryl group allows the use of this ligand system in the coordination chemistry of lanthanides and actinides [3].

Recently, another type of structural analogue of β-diketones – sulfonylamidophosphates (SAPhs), with the $S(O)_2NHP(O)$ functional core – has attracted the interest of researchers. This type of phosphoramide was first synthesized by Kirsanov and co-workers [4] and has been utilized in medicine as a bactericidal agent [5] and in agriculture as a pesticide [6]. In recent papers, we have reported the preparation, structural investigation and coordination behavior of some representative SAPh compounds. Moreover, the photophysical properties of a new series of NIR emitting lanthanide complexes based on these compounds have been studied [7]. It is important to note that *tetrakis*-complexes $[LnL_4]^-$ (where L is a SAPh ligand) usually contain eight coordinated lanthanide

ions [8], while the coordination sphere of the corresponding *tris*-complexes [LnL_3] is not saturated and therefore comprises additional solvent molecules. However, it is possible to obtain a six-coordinated tris-lanthanide complex without any solvent molecules when using ions with small radii. We report herein the structures of *N′*,*N″*-tetraethyl-*N ″*-(phenylsulfonyl)triamidophosphate (HL), LuL_3 (**1**) and $(AgL)_n$ (**2**) as part of our ongoing study on the coordination chemistry of sulfonylamidophosphates. In the current work, mass spectrometric data obtained by two different ionization techniques (ESI and MALDI) are presented. These methods are widely used for characterization of novel transition metal complexes, along with screening their bioactivity and a study of the interaction mechanism between metallo-drugs and biomolecules [9].

2. Results and discussion

2.1. Description of the structures

Crystallographic data for the compounds **HL**, **1** and **2** are summarized in Table 1.

Table 1. Selected crystallographic data for HL, LuL_3 (**1**) and $(AgL)_n$ (**2**).

Compound	**HL**	**1**	**2**
Formula	$C_{14}H_{26}N_3O_3PS$	$C_{42}H_{75}LuN_9O_9P_3S_3$	$C_{14}H_{25}AgN_3O_3PS$
Formula weight	347.42	1214.17	454.27
Temperature (K)	293(2)	293(2)	293(2)
Crystal system	monoclinic	hexagonal	monoclinic
Space group	$P2_1/c$	R3	$P2_1/c$
a (Å)	10.1911(2)	22.0475(7)	9.2211(2)
b (Å)	33.7250(11)	22.0475(7)	17.9073(4)
c (Å)	10.8284(3)	9.9007(3)	11.4105(2)
α (°)	90.00	90.00	90.00
β (°)	100.304(2)	90.00	100.598(2)
γ (°)	90.00	120.00	90.00
V ($Å^3$)	3661.64(17)	4167.9(2)	1852.02(7)
Z	8	3	4
μ (mm^{-1})	0.279	2.032	1.303
D_{calc} (g/cm^3)	1.260	1.451	1.629
$2\Theta_{max}$ (°)	50	60	60
Measured reflections	17427	12162	15422
Independent reflections	6122	5251	5335
R_{int}	0.022	0.020	0.018
Reflections with F>4σ(F)	5025	5200	3884
Parameters	496	206	212
R_1	0.076	0.019	0.032
wR_2	0.177	0.043	0.084
S	1.132	0.908	1.206
CCDC number	985455	985456	985457

Two molecules of HL (A and B) have been found in the asymmetric part of the unit cell. The bond lengths in the sulfonyl groups, S1A–O2A, S1A–O3A and S1A–N1A (Table 2), are similar to the corresponding values observed in $C_6H_5SO_2NHP(O)(OMe)_2$ [10]. These values depend on the substituent near the sulfur atom and are typical for sulfonylamide derivatives [11].

The P1A–O3A and P1A–N1A bond lengths for HL (Fig. 1, Table 2) have values which are typical for CAPhs with amide-type substituents [12]. The length of the P=O bond is influenced by the nature of the substituents attached to the phosphorus atom. The geometry around the phosphorus

atom in HL can be described as a distorted tetrahedron, with the N–P–N unequal angles centered at the phosphorus atom (Table 2).

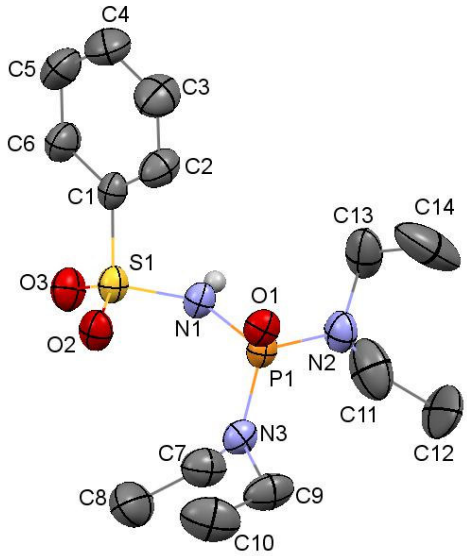

Fig. 1. The molecular structure of HL showing the atom numbering scheme (the disordering and the hydrogen atoms are omitted for clarity, except for those involved in the intramolecular hydrogen bond. The displacement ellipsoids are drawn at the 30% probability level.

Table 2. Selected bond lengths (Å) and bond angles (°) for HL.

Bond lengths (Å)	Mol. A	Mol. B	Bond angles (°)	Mol. A	Mol. B
S1–O2	1.421(3)	1.433(3)	O2–S1–O3	119.2(2)	119.2(2)
S1–O3	1.426(3)	1.420(4)	N1–S1–C1	104.3(2)	106.2(2)
S1–N1	1.624(4)	1.620(3)	O1–P1–N2	112.2(2)	114.3(2)
P1–N3	1.629(4)	1.627(4)	O1–P1–N1	111.9(2)	110.7(2)
P1–N1	1.693(3)	1.686(4)	O1–P1–N3	113.9(2)	114.4(2)
P1–N2	1.622(4)	1.622(4)	N3–P1–N1	105.4(2)	103.8(2)
P1–O1	1.479(3)	1.470(3)	N2–P1–N1	103.2(2)	107.0(2)
S1–C1	1.756(5)	1.778(4)	N2–P1–N3	109.5(2)	105.8(2)

Due to the steric effects, the values of the O–P–N angles in the derivatives of phosphoric acid are usually larger than those in the ideal tetrahedron (Table 2).

In the structure of HL, pseudo-torsion angles between the P=O bond and the nearest S=O bonds in the two independent molecules are –53.1 and –55.7°. A strong pπ-dπ conjugation between the oxygen atom of the sulfonyl group and the phosphorus atom can be established by comparison of the P…O(S) distances (3.06 Å in both molecules) with the sum of Van der Waals radii (3.12 Å) [13]. Strong hydrogen bonds, N–H···O=P (x, y, z) [d(H···O) = 1.98 Å, ∠N–H···O =166.5°] which connect the molecules into polymeric $(HL)_n$ chains, also have significant influence on the ligand conformation (Fig. 2, Table 3).

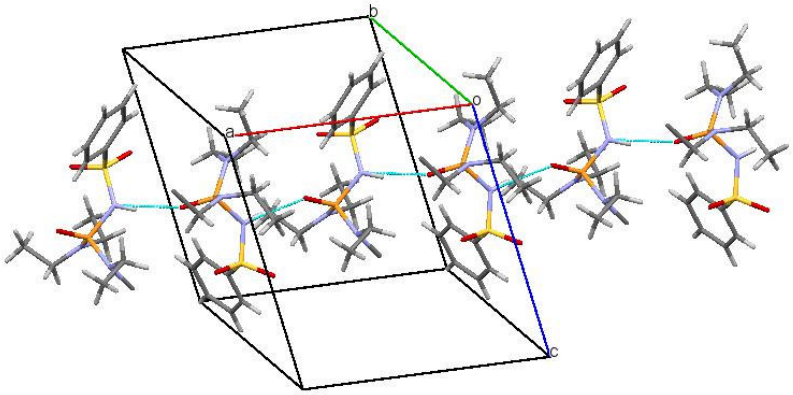

Fig. 2. The crystal packing of HL showing the N–H···O hydrogen bonds (dashed lines).

Table 3. Hydrogen bonding parameters (Å, °) for HL.

D–H···A	D–H	H···A	D···A	∠D–H···A
N1A–H1AA...O3B	0.86	1.98	2.819(4)	166.5
N1B–H1BA...O3A[(i)]	0.86	1.97	2.807(4)	163.9

[(i)] Symmetry code: x–1, y, z

The compound **1** is located in a special position, where the Lu atom is situated at the triad axis. The deprotonated ligands are coordinated to the Lu ion in the bidentate-chelate manner (Fig. 3). The elongation of the S=O (coordinated) and P=O bonds and shortening of the S–N and P–N bonds demonstrate the presence of strong π-conjugation within the $S(O)_2NP(O)$ fragment. The S=O bond length (for the non-coordinated fragments) remains practically the same as compared to the S=O bond length in the structure of HL.

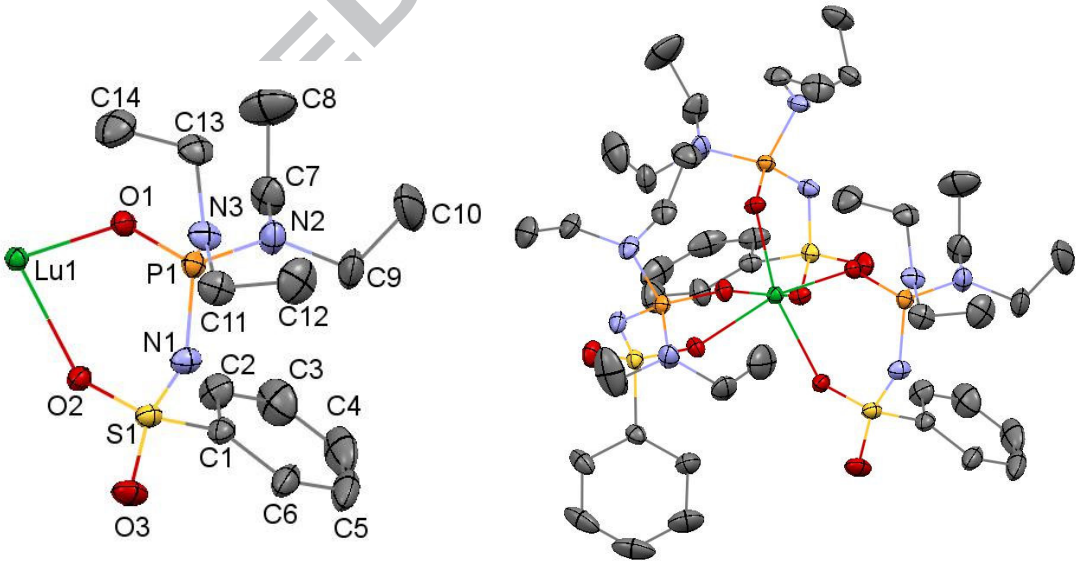

Fig. 3. The asymmetric part of the molecular structure of **1** showing the atom numbering scheme (A) and the whole complex with Lu (B). The displacement ellipsoids are drawn at the 30% probability level. The hydrogen atoms are omitted for clarity.

The Lu–O bond lengths, formed by sulfonyl and phosphoryl groups (Table 4), are in accordance to data for similar coordination compounds [8]. The shorter Lu–O(P) distance as compared to Lu–O(S) can be explained by the higher affinity of the phosphoryl group to the lanthanide ion (Table 4).

Table 4. Selected bond lengths (Å) and bond angles (°) for **1** and **2**.

Bond lengths (Å)		Bond angles (°)	
1			
Lu1–O1	2.147(1)	O1–Lu1–O2	80.75(5)
Lu1–O2	2.252(2)	O3–S1–O2	112.9(1)
S1–O3	1.431(2)	S1–N1–P1	124.9(1)
S1–O2	1.482(2)	O1–P1–N1	115.1(1)
S1–N1	1.545(2)	O1–P1–N3	112.1(1)
S1–C1	1.772(2)	O1–P1–N2	104.9(1)
P1–O1	1.510(2)	N1–P1–N2	112.6(1)
P1–N1	1.611(2)	N1–P1–N3	103.0(1)
P1–N2	1.631(2)	N2–P1–N3	109.3(1)
P1–N3	1.632(2)		
2			
Ag1–O1	2.152(2)	O1–Ag1–N1^{i}	163.75(8)
Ag1–O2	2.555(2)	O1–Ag1–O2	78.12(6)
Ag1–N1$^{(i)}$	2.157(2)	N1–Ag1–O2^{i}	118.12(7)
S1–O3	1.436(2)	O3–S1–O2	116.2(1)
S1–O2	1.443(2)	S1–N1–P1	124.6(1)
S1–N1	1.592(2)	O1–P1–N1	114.0(1)
S1–C1	1.766(3)	O1–P1–N3	116.4(1)
P1–N1	1.647(2)	O1–P1–N2	107.2(1)
P1–O1	1.493(2)	N2–P1–N3	105.3(1)
P1–N2	1.632(2)	N2–P1–N1	111.8(1)
P1–N3	1.647(2)	N3–P1–N1	101.9(1)

$^{(i)}$ Symmetry code: x, –y+1, z+0.5

The coordination environment of the Lu cation can be characterized as a distorted octahedron. The P=O and S=O bonds are facial. A weak interaction between the neighboring molecules exists through the non-coordinated oxygen atom of a sulfonyl group and one of the hydrogen atoms of the benzene rings.

The classical bidentate coordination mode of the sulfonylamidophosphate ligand *via* the oxygen atoms of the phosphoryl and sulfonyl groups was observed for **1**. In the case of complex **2**, the ligand is coordinated to the Ag ion in the tridentate manner, since the Ag(I) ion has a high affinity for N and O donors. As a result, one-dimensional polymeric chains along the *c* axis are formed in the complex $(AgL)_n$: the ligand is coordinated to one Ag cation in the bidentate manner *via* the oxygen atoms of the sulfonyl and phosphoryl groups, with an additional bridging coordination *via* the nitrogen atom to the neighboring Ag ion (Fig. 4). A short contact has been observed between the Ag ion and the oxygen atom of the sulfonyl group of the neighboring molecule (Ag1-O3 2.978Å).

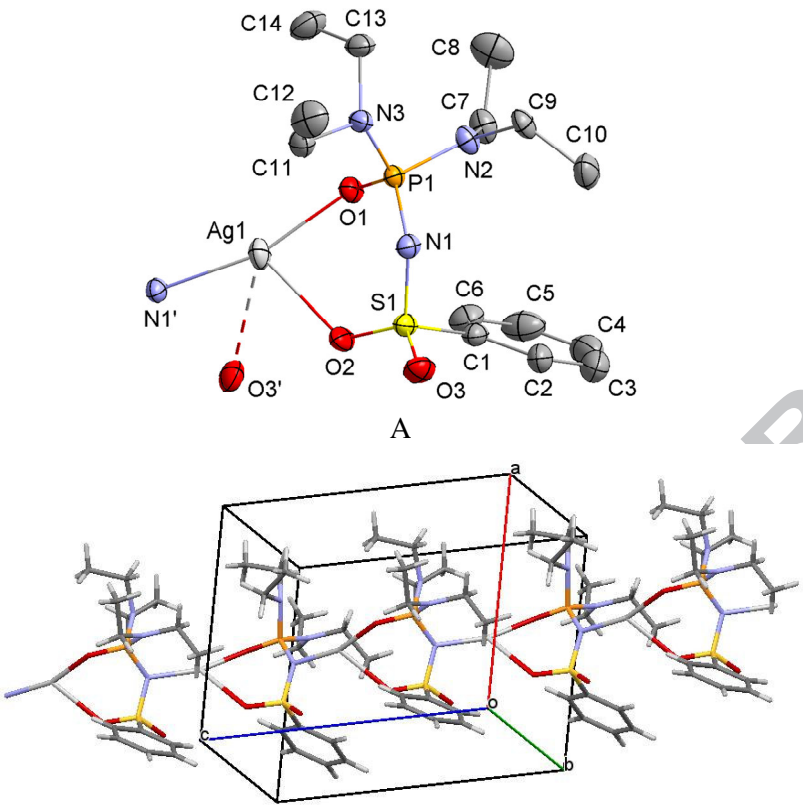

Fig. 4. The molecular structure of **2** showing the atom numbering scheme (A). The displacement ellipsoids are drawn at the 30 % probability level. The hydrogen atoms are omitted for clarity. A view of the one-dimensional chain of **2** along the *c* axis (B).

The coordination environment of the Ag cation can be characterized as a distorted triangle. The Ag1–N1 bond length is 2.157(2) Å. This value is smaller than the sum of ionic radii (2.26 Å) and can be explained by a significant covalent contribution to the Ag–N bond. Ag–N bond lengths of 2.169 and 2.135 Å were found for $Na[Ag(CCl_3C(O)NP(O)(OMe)_2)_2]\cdot CH_3CN$ [14] and $[Ag(C_{10}H_8N_2)(NH_3)]NO_3$ [15], respectively. The Ag1–O1 (phosphoryl group) distance is notably shorter than the Ag1–O2 (sulfonyl group) one (Table 4), with an O1–Ag1–N1 angle of 163.75(8)°. The O2–Ag1–N1 angle is 118.12(7)° due to an additional weak coordination contact with the sulfonyl oxygen atom O2.

For the analysis of the SAPh conformations, two parameters were chosen: a deviation of the six-membered chelate cycle from a mean plane which contains the O, P, S and O atoms (both oxygen atoms are coordinated to the metal ion), and the value of the pseudo-torsion angle between the P=O and S=O (coordinated) groups. Thus, in the structure of **1**, the value of the above-mentioned angle is 0.50°. The metallocycle adopts a boat conformation with puckering parameters S = 0.48, Θ = 61.6°, Ψ = 58.6°. The deviations of the N1 and Lu atoms from the mean plane of the remaining atoms of this cycle are 0.40 and 0.23 Å respectively. In the structure of **2**, the pseudo-torsion angle between the P=O and S=O (coordinated) bonds is equal to 26.1°, and the metallocycle adopts a twist-boat conformation with the puckering parameters S = 0.76, Θ = 87.4°, Ψ = 21.6°. The deviations of the N1 and Ag1 atoms from the O1–P1–O2–S1 mean plane are 0.393 and 0.688 Å, respectively. The coordination environment of the Ag ion is planar; the sum of the angles at this atom is equal to 360°. The deviation of the Ag1 atom from the O1–O2–N1 plane is 0.001 Å.

2.2. Spectroscopic characterization

The literature data was used to tentatively assign the absorption bands of the valence vibrations of the sulfonyl $\upsilon_{as}(SO_2)$, $\upsilon_s(SO_2)$ and phosphoryl $\upsilon(PO)$ groups [16]. The deprotonation of HL leads to a significant delocalization of the π-electron density in the SO_2NPO fragment and to the bathochromic shift of the valence vibrations in the spectra of the sodium salt NaL, **1** and **2** as compared to HL, by the values of $\Delta\upsilon_{as}(SO_2)$ = 60–120 cm^{-1}, $\Delta\upsilon_s(SO_2)$ = 25–40 cm^{-1} and $\Delta\upsilon(P{=}O)$ = 35–60 cm^{-1}.

The broad absorption band located at 2950–3100 cm^{-1} in the IR spectrum of HL was tentatively assigned to the amide group $\upsilon(N–H)$. This band is missing in the spectra of the sodium salt and complexes **1** and **2**, which is evidence of ligand deprotonation.

2.3. Laser desorption/ionization (LDI MS) and ESI MS of $(AgL)_n$

The mass spectrum fragmentation of the complex with the formula $(AgL)_n$ in the mass range of 320–850 Da is shown in Fig. S1, Supporting Information. The most intensive peak, with a *m/z* ratio of 346.6, can be assigned to the deprotonated ligand. The peaks with *m/z* values of 453.9, 563.5, and 802.1, which can be assigned to associates of silver and the ligand with various structures, are summarized in the Table S1, Supporting Information.

The peaks with *m/z* values of 390.7 and 422.5, located in the negative part of the spectrum, contain one silver atom and various fragments of the ligand molecule. The series of peaks with *m/z* values of 490.6, 517.7, 532.7, 620.8 and 631.8 correspond to derivatives of an ion-molecular associate with the formula $[Ag_2L]^-$. All of these fragments contain two silver atoms. Further series of peaks with *m/z* values over 650 (659.9, 715.9, 750.9) correspond to silver-containing fragments of an ion-molecular associate with the formula $[AgL_2]^-$. All of these fragments are formed by acceptance of an electron, in contrast to the fragment with the formulae $[L]^-$, which is formed by deprotonation of the starting compound. Thus, introducing the silver atom into the molecule changes the ionization mechanism.

Peaks which correspond to ligand fragments participating in the association processes are observed in the low-molecular area of the mass spectra.

It should be noted that the fragmentation of the complex studied in the negative mode is more intensive in contrast to that in positive mode [17], where association processes due to acceptance of protons and metal atoms play the main role.

Thus, we can suppose a two-step mechanism of the complex fragmentation, with the first step including cleavage of the bonds between the basic units of the polymeric structure and participation of different numbers of the silver atoms and the ligand residues (forming ion-molecular associates with various structures). Another explanation of the fragmentation pathway includes formation of the described unstable fragments already in the starting sample. The high ionization capability of those fragments leads to high intensity of the corresponding peaks, in contrast to the less intensive peaks related to the ion-molecular associates (more stable structures). The second step can be explained by the interaction of ligand fragments with various complex associates in the gas phase under the mass spectrometric conditions.

In the ESI mass spectrum of the studied complex, a small number of peaks is observed, the most intensive one corresponding to $[L]^-$ (Table S2, Supporting Information). This feature of the mass spectrum can be explained by the "soft" ionization mechanism of the ESI MS method, which reduces fragmentation. The series of peaks with *m/z* values about 238, 291 and 528, and at 538.1 correspond to fragments of the ligand and its associates which do not contain silver. The series of peaks with *m/z* values about 498, 606 and 690 correspond to ion-molecular associates containing two to four silver atoms and various fragments of the ligand molecule. The pesence of such fragments in the negative mode mass spectrum confirms the high propensity of the complex studied towards association in the gas phase.

We suppose that the studied complex $(AgL)_n$ is fragmented and ionized under the ESI conditions due to association of the ligand mainly with the metal ions.

The possibility of the formation of different associates observed in the two mass-spectroscopic studies was confirmed by quantum chemical calculations (see below).

2.4. DFT calculations

Based on the values of the full energy of the neutral ligand and its anion (Fig. 5), the energy of deprotonation was calculated (1.063 a.u. or 2792.6 kJ/mol). At 298.15 K, the Gibbs free energy of this process is equal 2746.6 kJ/mol; therefore, HL can be considered as a weak acid. Nevertheless, it forms sodium and silver salts relatively simply.

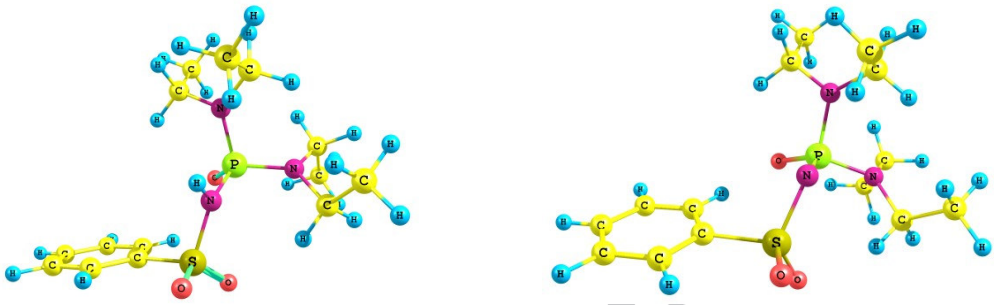

A B

E_{full} = –188.96140 a.u. E_{full} = –187.8980776 a.u.

Fig. 5. The calculated geometry of HL (A) and L^- (B)

In the silver salt crystals, a chain structure with the ligand anions and the silver cations alternating each other can be outlined. We calculated the spatial structure and total energy of the dimer and monomer associates of the silver salt (Figs. 6 and 7). Considering the total energy of the silver cation (-145.996 a.u.), it is possible to determine the affinity for the anion (0.768 a.u. or 2016.4 kJ/mol) and for the monomer salt (0.126 a.u. or 330.3 kJ/mol). The energy of dimerization of the silver salt is –0.045 a.u. (–117.1 kJ/mol).

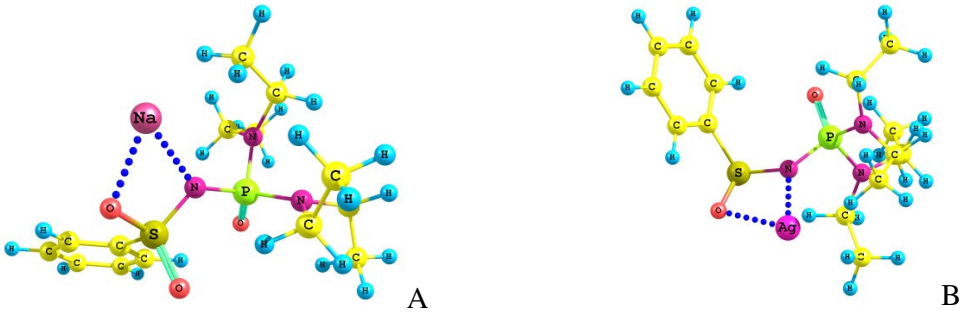

A B

E_{full} = –188.62530 a.u. E_{full} = –334.66150 a.u.

Fig. 6. The calculated geometries of NaL (A) and AgL (B)

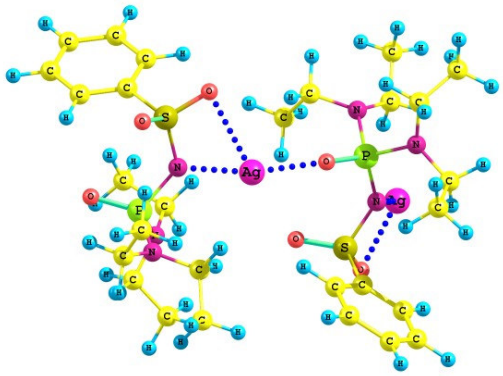

A

E_{full} = –669.36761 a.u.

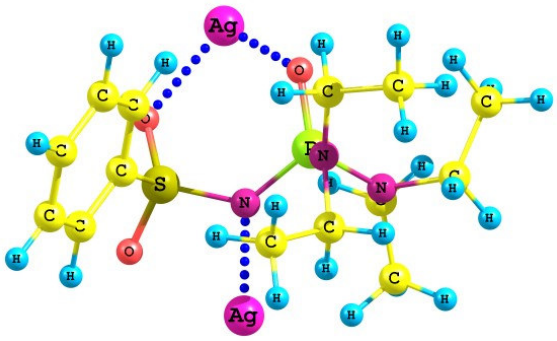

B

E_{full} = –480.78304 a.u.

Fig. 7. The calculated geometries of the dimer Ag_2L_2 (A) and the Ag_2L^+ (B) associate

It is well-known that the HOMO energy describes the electron donor properties, whereas the LUMO energy characterizes the electron acceptor properties [18]. The HOMO–LUMO orbital schemes for the compounds studied are shown in Fig. 8. In HL, the electron density of the HOMO is localized mainly at the P=O, both C–N bonds, C–C and C–N bonds (ethyl substituents). In the case of the LUMO, the orbital is located at the S=O and C–S bonds and the C–C bonds of the phenyl ring. The $\Delta_{HOMO–LUMO}$ value is 232.466 nm. For NaL and AgL, the electron density of the HOMO is localized similarly to that of HL. The LUMO orbital is located at the Na and Ag ions. The $\Delta_{HOMO–LUMO}$ gap is 271.3 nm for NaL and 792.4 nm – for AgL.

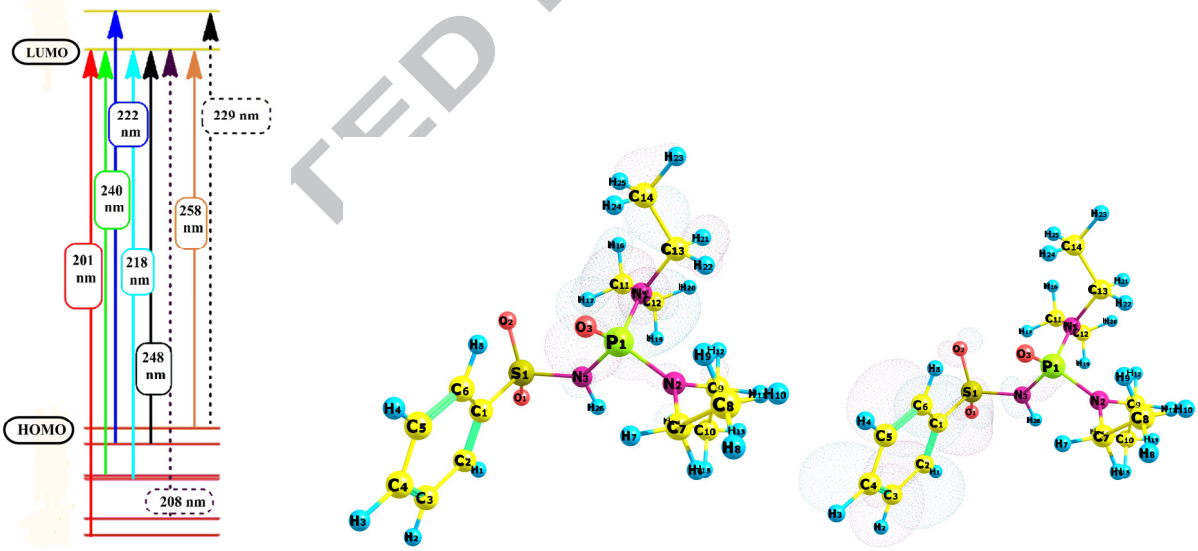

(A)

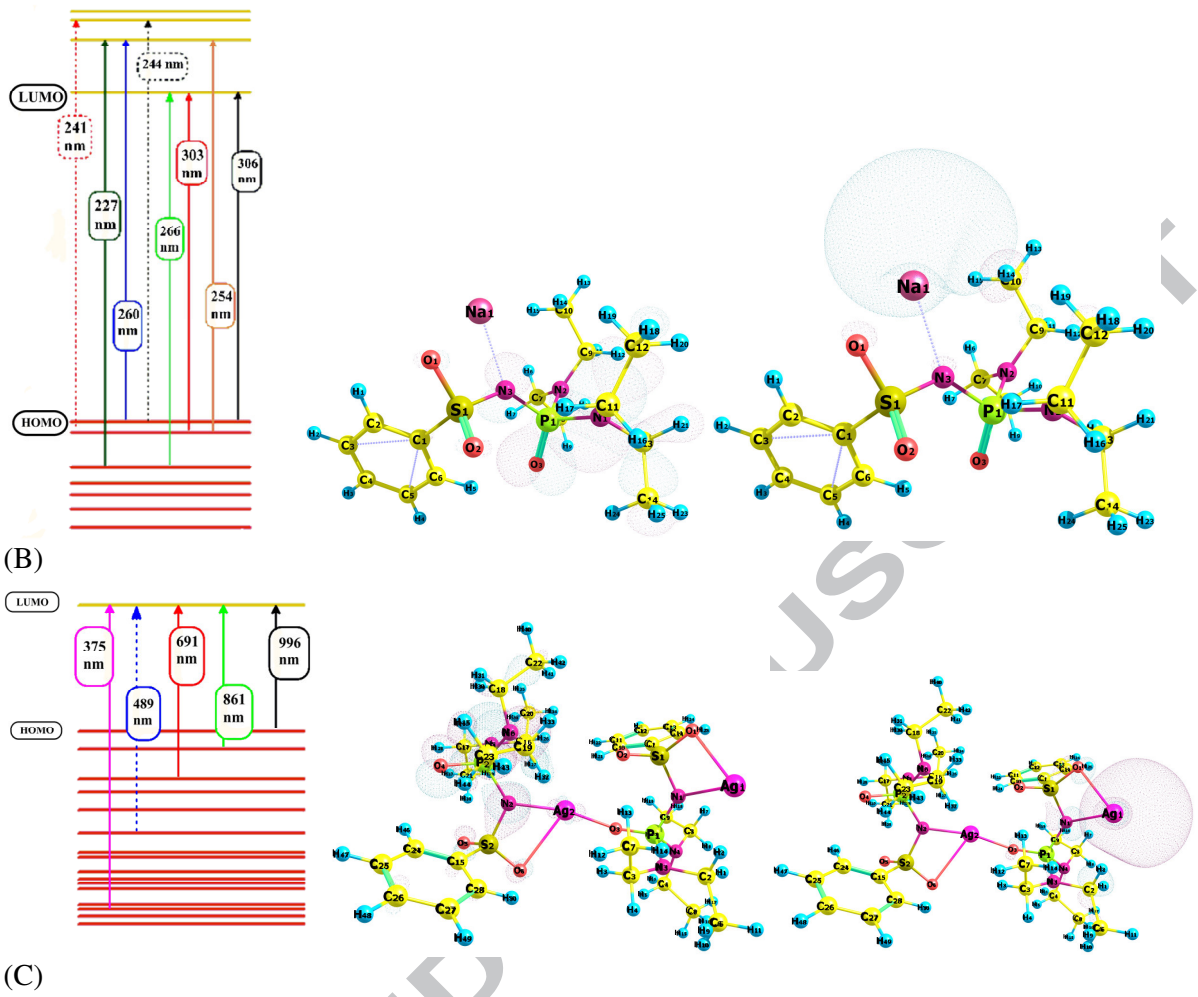

Fig. 8. The theoretically calculated electronic transitions and HOMO–LUMO orbital schemes for HL (A), NaL (B) and Ag_2L_2 (C)

The presence of conjugation in the chelate fragment O=S–N–P=O is confirmed by the analysis of bond orders and effective charges on the atoms. The bond order of S=O decreases in the series: HL, Ag_2L_2, AgL, NaL and anion L^-. The bond order of P=O decreases from the largest value for HL to the smallest for L^-. On the contrary, the S–N and N–P bond orders increase in AgL and NaL as compared to that of HL. Meanwhile, conjugation of the benzene ring and terminal NEt_2 group with this fragment decreases. As a result, the effective charges increase on the oxygen atoms that are in contact with the metal ion (Tables 5 and 6).

Table 5. The calculated bond orders.

	HL	L^-	NaL	AgL	Ag_2L_2 fragment
C–S	0.638	0.287	0.615	0.63	0.599
S=O[(i)]	1.710, 1.718	1.212, 1.113	1.710, 1.369*	1.733, 1.434*	1.681, 1.461*
S–N	0.765	0.712	0.892	0.905	0.915
N–P[(ii)]	0.891	1.01	1.047	0.979	1.042
P=O	1.934	1.473	1.860	1.907	1.670
P–N[(iii)]	1.037, 1.060	0.658, 0.670	0.941, 0.996	0.998, 0.996	0.972, 1.110
Na,Ag–O			0.221	0.191	0.224, 0.070
Na,Ag–N			0.270	0.340	0.360

[(i)] The coordinated S=O group.
[(ii)] Between the SO_2 and P=O groups.

[iii] The terminal NEt_2 group.

Table 6. The calculated Mulliken charges.

	O(S)	O(S)	N	O(P)
HL	–0.334	–0.339	–0.413	–0.426
LA	–0.471	–0.494	–0.474	–0.562
NaL	–0.349	–0.474[i]	–0.460	–0.448
AgL	–0.333	–0.405[i]	–0.479	–0.438
AgLAgK	–0.364	–0.387[i]	–0.446	–0.490
Ag_2L_2 fragment	–0.296	–0.389[i]	–0.453	–0.446

[i] The coordinated S=O group

3. Conclusions

The conformation of the deprotonated form of the SAPh type ligand *N*-[bis(diethylamino)phosphoryl]benzenesulfonamide (HL) within the coordination compounds $(AgL)_n$ and LuL_3 depends significantly on the nature of the metal ion. In the case of the Lu complex, the usual coordination mode *via* the oxygen atoms of the sulfonyl and phosphoryl groups occurs, whereas in the Ag complex, the chelate coordination of the SAPh ligand is accompanied by a bridging function of the imide nitrogen atom. Such a type of coordination mode is observed for *d*-metal complexes for the first time. It could be noted that no water or other solvent molecules are found in the structure. The compounds are thermally stable up to 310 °C (LuL_3) and 220 °C ($(AgL)_n$); the decomposition starts upon further heating. ESI and MALDI mass-spectroscopic studies show rather complicated pathways for the fragmentation process, but the major peaks can be assigned. DFT calculations show the possibility of dimer formation, which was observed in the mass spectra.

4. Experimental

4.1. Materials and methods

All reagents were purchased from commercial sources and used without purification. IR samples were prepared as KBr pellets (in the case of the complex **2**, nujol was used), and the spectra were recorded with a Perkin-Elmer Spectrum BX spectrometer in the range 4000-400 cm^{-1}. ^1H (400 MHz) and ^{31}P NMR (162.1 MHz) spectra were recorded on a Varian Mercury 400 NMR spectrometer. The thermal stabilities of **1** and **2** have been determined between 20 and 1000 °C in air with a heating rate of 10 °C min^{-1} by thermal gravimetric (TG) and differential thermal analyses (DTA).

The samples for the MALDI-TOF analysis were prepared as follows: 1 mg of the complex was dissolved in acetonitrile (1 mL). Aliquots of the solution were applied to the steel tips and dried. MS analysis was performed by the method of laser desorption/ionization on an Autoflex II (Bruker Daltonics, Germany) mass spectrometer with a nitrogen laser (λ = 337 nm). Experiments were carried out in the reflectron mode for negative ions in the *m/z* range from 50 to 2000 a.m.u. The resulting mass spectra were obtained by acquiring the data of 150 laser shots and processing by the software FlexAnalysis (Bruker Daltonics, Germany).

LC/MS analysis was performed with an Agilent 1200 HPLC equipped with a single-quadrupole MSD Agilent G1956B and Multimode ion source Agilent G1978A (Agilent Technologies, USA). Signals were detected in the SCAN mode 50–500 *m/z*, fragmentor variable – from 70 to 300 V. Ionization - MM-ESI in the negative mode, drying gas flow 5.0 L/min, nebulizer pressure 60 psi, drying gas temperature 300 °C, vaporizer temperature 200 °C.

Quantum-chemical calculations were carried out with Firefly v.8.1.1 software [19] using DFT [20] with the hybrid three-parameter Becke–Lee–Yang–Parr functional (B3LYP) [21] with SBKJC

[22] basis sets to compare the molecular (experimental and calculated) structure and vibrational wave numbers. The wave number values computed contain known systematic errors [23], and therefore, we have used the scaling factor values of 0.967 for the B3LYP functional.

Energetic effects of the condensation reactions were calculated according to the formula

$$\Delta E = \Sigma E_{full\ (reaction\ products)} - \Sigma E_{full\ (precursors)}$$

and the results are given in kJ / mol, based on the relation 1 a.u. = 2625.5 kJ / mol.
The accuracy of the energy parameters calculations was 10^{-5} a.u. (26 J / mol).
Electronic absorption spectra were calculated using electron density functional theory TD–DFT.

All crystallographic measurements were performed at room temperature on an XCalibur-3 diffractometer (graphite monochromator MoK_α radiation, $\lambda(MoK_\alpha)$ = 0.71073 Å, CCD-detector, ω-scans). The structures were solved by direct methods using the SHELXTL package [24]. Positions of the hydrogen atoms were located from the electron density difference maps and refined by the "riding" model with $U_{iso} = nU_{eq}$ of the non-hydrogen atom bonded with given hydrogen atom (n = 1.5 for methyl groups and n = 1.2 for other hydrogen atoms). The ethyl fragments at the nitrogen atoms in the structure of HL were disordered, each one over two sites, with refined occupancy factors 0.600(13) (for C10A) and 0.400(13) (for C10B); 0.745(48) (for C12A) and 0.26 (48) (for C12B); 0.602(16) (for C13A, C14A) and 0.400(16) (for C13B, C14B); 0.559(10) (for C7C, C7D) and 0.441(10) for C8C, C8D); 0.510(11) (for C11C, C12C, C13C, C14C) and 0.490(11) (for C11D, C12D, C12D, C14D).

4.1 Synthesis

HL was synthesized according to the Scheme 1.

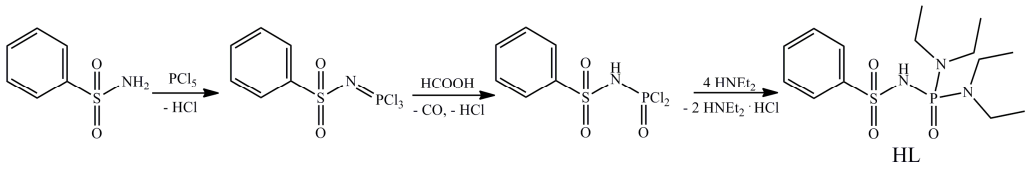

Scheme 1.

Synthesis of HL. A solution of diethylamine (53.4 mL, 1.035 mol) in dioxane (100 mL) was placed into a three-neck round-bottomed flask equipped with a thermometer and cooled down to 5 ºC. A solution of (phenylsulfonyl)phosphoramidic dichloride ($C_6H_5SO_2NPOCl_2$) (63.5 g, 0.250 mol) [10] in dioxane (100 mL) was added dropwise to the diethylamine solution under stirring. The temperature was kept below 10 ºC. After the addition was complete, stirring was continued for 1 h, and then the mixture was left for 3 h. The solvent was then evaporated and the residue was dried in vacuum. The resulting mixture of HL and $HN(C_2H_5)_2 \cdot HCl$ was dissolved in water and the solution was acidified with HCl_{conc} to pH ≈ 2. The final product precipitated as a yellowish crystalline powder which was recrystallized from ethanol to give a white crystalline powder (90 g, 80%), mp = 120 °C. HL is soluble in acetone, methanol, ethanol, 2-propanol, DMF and DMSO, and insoluble in non-polar solvents and water. IR (KBr, ν cm^{-1}): 2980 (NH), 1222 (PO); 1323, 1177 (SO_2) (Fig. S2, Supporting Information). ^{1}H NMR (DMSO-d_6, 400 MHz, 25 °C) δ, ppm: 2.92 (m, 8H, CH_2); 1.02 (t, 12H, CH_3, J_{P-H} = 7.2 Hz); 7.95 (H_α, J_{H-H} = 8 Hz, C_6H_5), 7.55 ($H_{\beta,\gamma}$, C_6H_5). ^{31}P NMR (162.1 MHz, DMSO-d_6) δ, ppm: 6.66 (m, $^3J_{P-H}$=6.5 Hz).

The sodium salt NaL was prepared by the reaction of equimolar amounts of sodium methoxide and HL in 2-propanol medium. The resulting solution was evaporated to dryness and the fine-crystalline powder was collected. IR (KBr, ν cm^{-1}): 1130 (PO); 1210, 1040, 1075 (SO_2) (Fig. S3, Supporting Information). ^{1}H NMR (DMSO-d_6, 400 MHz, 25 °C) δ, ppm: 2.86 (8H, CH_2); 0.88 (t, 12H, CH_3, J_{P-H} = 6.8 Hz);7.77 (H_α, J_{P-H} = 8 Hz, C_6H_5), 7.33 ($H_{\beta,\gamma}$, C_6H_5). ^{31}P NMR (162.1 MHz, DMSO-d_6) δ, ppm: 10.16 (m, $^3J_{P-H}$=11.3 Hz).

Synthesis of 1. $Lu(NO_3)_3 \cdot 4.78H_2O$ (0.14 g, 0.31 mmol) was dissolved in *i*-PrOH (10 mL), and the solution was added to a NaL solution (0.35 g, 0.95 mmol) in a mixture of *i*-PrOH and CH_3OH (1:1, 20 mL). After 20 min of stirring, the precipitate of $NaNO_3$ was filtered and washed with small amount of cold *i*-PrOH. The resulting mother liquor was left for crystallization in a vacuum desiccator. Colorless crystals of LuL_3 were collected after several days. IR (KBr, ν cm^{-1}): 1164 (PO); 1194, 1113 (SO_2) (Fig. S4, Supporting Information). ^{1}H NMR (DMSO-d_6, 400 MHz, 25 °C) δ, ppm: 2.49 (8H, CH_2); 0.89 (m, 12H, CH_3, J_{P-H}= 6.8 Hz); 7.89 (H_α, J_{P-H} = 7.6 Hz, C_6H_5); 7.37 ($H_{\beta,\gamma}$, C_6H_5).

Synthesis of 2. $AgNO_3$ (0.097 g, 0.56 mmol) was dissolved in acetonitrile (10 mL), and the solution was added to a NaL solution (0.21 g, 0.56 mmol) in *i*-PrOH (10 mL). After 30 min, the precipitate of $NaNO_3$ was filtered and washed with small amount of acetonitrile. The resulting clear solution was left for crystallization in a dark vacuum dessicator. Colorless crystals of $(AgL)_n$ were collected after several days. The complex **2** is light sensitive. IR (nujol mull, ν cm^{-1}): 1150 (PO); 1270, 1090, 1060 (SO_2) (Fig. S5, Supporting Information). ^{1}H NMR (DMSO-d_6, 400 MHz, 25 °C): δ 2.65 (8H, CH_2); 0.64 (t, 12H, CH_3, J_{P-H}= 6.8 Hz); 7.56 (H_α, C_6H_5), 7.05 ($H_{\beta,\gamma}$, C_6H_5).

4.2. Thermal gravimetric analysis

TGA was carried out to evaluate the thermal stabilities of **1** and **2**. As can be seen (Fig. S6, Supporting Information), the TGA curve of **1** does not show any weight loss until heating to 310 °C, which suggests that this compound does not contain solvent or water molecules. The largest weight loss (approximately 77% of the starting weight) occurs in the range 310–410 °C, which might be attributed to the decomposition of LuL_3. The decomposition process is completed around 920 °C, resulting in lanthanide polyphosphate as the final product (approximately 15% of the starting weight). The TGA curves indicate that **2** is stable up to 220 °C, which suggests that this compound also does not contain solvent or water molecules. Further destruction of $(AgL)_n$ occurs in three steps. The temperature range and weight loss percentages (shown in brackets) for the first decomposition step are 220-310 °C (19 %, decomposition of the organic ligand), for the second step – 310-350 °C (38%, final oxidation decomposition of the organic ligand) and for the third – 350-800 °C (14%, polyphosphate conversion). The calculated metal content (28.7%) for the residue as well as analysis of its IR spectrum testify Ag_3PO_4 as the residue's main component.

Appendix A. Supplementary data

Crystallographic data for the structures reported in this paper have been deposited with the Cambridge Crystallographic Data Center. The CCDC numbers are 985455, 985456 and 985457. Copies of the data can be obtained free of charge *via* www.ccdc.cam.ac.uk/conts/retrieving.html or from the CCDC, 12 Union Road, Cambridge CB2 1EZ, UK; fax: +44 1223 336033; E-mail: deposit@ccdc.cam.ac.uk.

Acknowledgments

We are grateful to Dr. A.M. Ostapchuk (Danylo Zabolotny Institute of microbiology and virology) for his help with ESI mass spectroscopy.

References

[1] (a) V.P. Morgalyuk, A.M. Safiulina, I.G. Tananaev, E.I. Goryunov, I.B. Goryunova, N.G. Molchanova, T.V. Baulina, Dokl. Chem. 403 (2005) 126-128;
(b) E.I. Goryunov, T.V. Baulina, I.B. Goryunova, E.D. Savin, P.V. Petrovskii, E.I. Matrosov, E.E. Nifant'ev, Dokl. Chem. 419 (2008) 87-90;

(c) A.M. Safiulina, E.I. Goryunov, A.A. Letyushov, I.B. Goryunova, S.A. Smirnova, A.G. Ginzburg, I.G. Tananaev, E.E. Nifant'ev, B.F. Myasoedov, Mendeleev Commun. 19 (2009) 263-265.
[2] (a) K. Jaroslav, F. Swerdloff, US Patent 4 517 003 (1985);
(b) K.D. Grimes, Y.-J. Lu, Y.-M. Zhang, V.A. Luna, J.G. Hurdle, E.I. Carson, J. Qi, S. Kudrimoti, C.O. Rock, R.E. Lee, ChemMedChem. 3 (2008) 1936-1945;
(c) L.A Adams, R.J. Cox, J.S. Gibson, M.B. Mayo-Martin, M. Walter, W. Whittingham, Chem. Commun. 18 (2002) 2004-2005;
(d) N.G. Zabirov, O.K. Pozdeev, F.M. Shamsevaleev, R.A. Cherkasov, G.H. Gilmanova, J. Pharm. Chem. 23 (1989) 423-425;
(e) K. Gholivand, F. Ghaziani, Z. Shariatinia, N. Dorosti, M. Mirshahi, S. Sarikhani, Med. Chem. Res. 21 (2012) 2185-2195;
(f) K. Gholivand, F. Molaei, N. Oroujzadeh, R. Mobasseri, H. Naderi-Manesh, Inorg. Chim.Acta. 423 (2014) 107-116.
[3] (a) J. Legendziewicz, G. Oczko, V. Amirkhanov, R. Wiglusz, V. Ovchynnikov, J. Alloys Compd. 300-301 (2000) 360-365;
(b) T.Q. Ly, J.D. Woollins, Coord. Chem. Rev. 176 (1998) 451-481;
(c) V.V. Skopenko, V.M. Amirkhanov, T.Yu. Sliva, I.S. Vasilchenko, E.L. Anpilova, A.D. Garnovskii, Usp. Khim. 793 (2004) 797-813;
[4] A.V. Kirsanov, V.I. Shevchenko, Russ. J. Gen. Chem. 24 (1954) 882-887.
[5] (a) K. Xu, C. Angell, Inorg. Chim. Acta 298 (2000) 16-23;
(b) K. Gholivand, N. Oroujzadeh, F. Afshar, J. Organomet. Chem. 695 (2010) 1383-1391.
[6] S. Kishino, S.Saito, US Patent 4 161 524 (1979).
[7] (a) O.V. Moroz, V.A. Trush, K.O. Znovjyak, I.S. Konovalova, I.V.Omelchenko, T.Yu. Sliva, O.V. Shishkin, V.M. Amirkhanov, J. Mol. Struct. 1017 (2012) 109-114;
(b) P. Gawryszewska, O.V. Moroz, V.A. Trush, D. Kulesza, V.M. Amirkhanov, J. Photochem. Photobiol. A: Chem. 217 (2011) 1-9;
(c) P. Gawryszewska, O.V. Moroz, V.O. Trush, V.M. Amirkhanov, T. Lis, M. Sobczyk, M. Siczek, ChemPlusChem 77 (2012) 482-486;
(d) D. Kulesza, M. Sobczyk, J. Legendziewicz, O. Moroz, V. Amirkhanov, Struct. Chem. 21 (2010) 425-438.
[8] (a) O.V. Moroz, S.V. Shishkina, V.A. Trush, T.Yu. Sliva, V.M. Amirkhanov, Acta Cryst. E63 (2007) m3174-m3176;
(b) I.O. Shatrava, T.Yu. Sliva, V.A. Ovchynnikov, I.S. Konovalova, V.M. Amirkhanov, Acta Cryst. E66 (2010) m397-m398.
[9] M. Petkovic, T. Kameva, Metallomics 3 (2011) 550-565.
[10] O.V. Moroz, V.A. Trush, I.S.Konovalova, O.V. Shishkin, Yu.S. Moroz, S. Demeshko, V.M. Amirkhanov, Polyhedron 28 (2009) 1331-1335.
[11] H.-B. Burgi, J.D. Dunitz, Struct. Correlation VCH, Weinheim 1997.
[12] V. Amirkhanov, V. Ovchynnikov, V. Trush, P. Gawryszewska, L.B. Jerzykiewicz, in: P. Gawryszewska, P. Smolenski (Eds.), Ligands Synthethis, Characterisation and Role in Biotechnology, Nova Science Publishers, New York, 2014, pp. 199–249.
[13] V. Mizrahi, T.A. Modro, Cryst. Struct. Comm. 11 (1982) 627-631.
[14] V.O. Trush, K.V. Domasevich, V.M. Amirkhanov, DAN Ukr. 7 (2007) 147-151.
[15] D. Sun, N. Zhang, G.-G. Luo, R.-B. Huang, L.-S.Zheng, Acta Cryst. C66 (2010) m75-m78.
[16] (a) S. Boudjabi, G. Dewynter, J.-L. Montero, Synlett. 5 (2000) 716-718;
(b) S. Zhu, J. Zhang, B. Xu, J. Fluorine Chem. 78 (1996) 183-185.
[17] I.O. Shatrava, O.V. Severinovskaya, V.A. Ovchynnikov, V.M. Amirkhanov, V.A. Pokrovskiy, Chem. Phys. & Technol. of Surface. 7 (2016) 31-34.
[18] X.T. Xavier, I.H. Joe, Spectrochim Acta A 79 (2011) 322-337.

[19] A. Granovsky (2015) Firefly version 8.1.1, build number 9295, Compiled 31 Aug 2015. http://classic.chem.msu.su/gran/firefly/index.html
[20] R.G. Parr, W. Yang, Density - functional theory of atoms and molecules. Oxford University Press.; Oxford 1989.
[21] (a) A.D. Becke, J. Chem. Phys. 98 (1993) 5648-5652;
(b) C. Lee , W. Yang, R.G. Parr, Phys. Rev. B 37 (1998) 785-789;
(c) B. Miehlich, A. Savin, H. Stoll, H. Preuss, Chem. Phys. Lett. 157 (1989) 200-206.
[22] (a) SBKJC ECP EMSL Basis Set Exchange Library 20 Oct 2015: H -He, J.S. Binkley, J.A. Pople, W.J. Hehre, J. Am. Chem. Soc. 102 (1980) 939-947;
(b) Li - Ar, W.J. Stevens, H. Basch, M. Krauss, J. Chem. Phys. 81 (1984) 6026-6033;
(c) K - Rn, W.J. Stevens, M. Krauss, H. Basch, P.G. Jasien,Can. J. Chem. 70 (1992) 612-630;
(d) Ce - Lu, T.R. Cundari, W.J. Stevens, J. Chem. Phys. 98 (1993) 5555-5565;
[23] J.P. Merrick, D. Moran, L. Radom, J. Phys. Chem.A 11 (2007) 11683-11700.
[24] G.M. Sheldrick. SHELXL97 and SHELXS97, Program for X-ray Crystal Structure Refinement, University of Guttingen, Germany 1997.

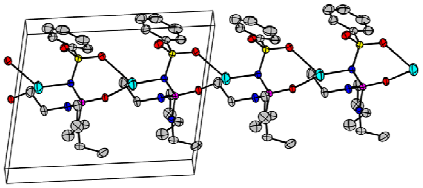

We report the synthesis of two novel complexes, LuL_3 and $(AgL)_n$, based on a sulfonylamidophosphate ligand. The X-ray single crystal structures of the ligand and the complexes were determined, showing two different coordination modes in the complexes. ESI and MALDI mass-spectroscopic studies of $(AgL)_n$ show rather complicated pathways for the fragmentation process. The results were supported by DFT calculations.